IJCRT.ORG ISSN : 2320-2882

INTERNATIONAL JOURNAL OF CREATIVE RESEARCH THOUGHTS (IJCRT)

An International Open Access, Peer-reviewed, Refereed Journal

Diabetic Retinopathy Detection using Machine Learning

AbhimanyuGadhave[1], Ashwini Wadekar[2] ,Prashant Patil [3], Mahesh Tathe[4], Nageshwar Jadhav[5], Krushna Raut[6]

[1]Department of Computer Engineering, Suman Ramesh Tulsiani Technical Campus- Faculty of Engineering.Khamshet

[2]Department of Computer Engineering, Suman Ramesh Tulsiani Technical Campus- Faculty of Engineering.Khamshet

[3]Department of Computer Engineering, Suman Ramesh Tulsiani Technical Campus- Faculty of Engineering.Khamshet

[4]Department of Computer Engineering, Suman Ramesh Tulsiani Technical Campus- Faculty of Engineering.Khamshet

[5]Department of Computer Engineering, Suman Ramesh Tulsiani Technical Campus- Faculty of Engineering.Khamshet

[6]Department of Computer Engineering, Suman Ramesh Tulsiani Technical Campus- Faculty of Engineering.Khamshet

ABSTRACT : Recently, the Internet of Things (IoT) and computer vision technologies find useful in different applications, especially in healthcare. IoT driven healthcare solutions provide intelligent solutions for enabling substantial reduction of expenses and improvisation of healthcare service quality. At the same time, Diabetic Retinopathy (DR) can be described as permanent blindness and eyesight damage because of the diabetic condition in humans. Accurate and early detection of DR could decrease the loss of damage. Computer-Aided Diagnoses (CAD) model based on retinal fundus image is a powerful tool to help experts diagnose DR. Some traditional Machine Learning (ML) based DR diagnoses model has currently existed in this study. The recent developments of Deep Learning (DL) and its considerable achievement over conventional ML algorithms for different applications make it easier to design effectual DR diagnosis model. With this motivation, this paper presents a novel IoT and DL enabled diabetic retinopathy diagnosis model (IoTDL-DRD) using retinal fundus images. The presented Internet of Things Deep Learning–Diabetic Retinopathy Diagnosis (IoTDL-DRD) technique utilizes IoT devices for data collection purposes and then transfers them to the cloud server to process them. Followed by, the retinal fundus images are preprocessed to remove noise and improve contrast level. Next, mayfly optimization based region growing (MFORG) based segmentation technique is utilized to detect lesion regions in the fundus image. Moreover, densely connected network (DenseNet) based feature extractor and Long Short Term Memory (LSTM) based classifier is used for effective DR diagnosis. Furthermore, the parameter optimization of the LSTM method can be carried out by Honey Bee Optimization (HBO) algorithm. For evaluating the improved DR diagnostic outcomes of the IoTDL-DRD technique, a comprehensive set of simulations were carried out. A wide ranging comparison study reported the superior performance of the proposed method.

INDEX TERMS: Computer aided diagnosis, deep learning, diabetic retinopathy, fundus images, honey bee optimization.

I.INTRODUCTION

Diabetic Retinopathy is a complication that affect the eye due to the result of high blood glucose called diabetes. It can cause vision loss and in severe condition can lead to complete blindness. Early symptoms of diabetic retinopathy includes blurred vision, darker areas of vision, eye floaters and difficulty in perceiving colours. Proper detection of diabetic retinopathy in early stage is extremely

important to prevent complete blindness. Of an estimated 285 million people with diabetes mellitus worldwide, approximately one third have signs of diabetic retinopathy. Globally the number of people affected with diabetic retinopathy will increase from 126.6 million in 2010 to 191.0 million by 2030. Non Proliferative Diabetic Retinopathy (NPDR) is an early stage of disease in retina where tiny red spots occur. These tiny spots may represent haemorrhage and abnormal pouching of blood vessels represents microaneurysms. The lining of these blood vessels can become damaged enough to allow leakage of fluid and fatty material called exudates. Available physical tests to detect diabetic retinopathy includes pupil dilation, visual acuity test, optical coherence tomography, etc. But they are time consuming and patients need to suffer a lot. This paper focuses on automated computer aided detection of diabetic retinopathy using machine learning hybrid model by extracting the features haemorrhage, microaneurysms and exudates. The classifier used in this proposed model is the hybrid combination of SVM and KNN.

II. LITERATURE REVIEW

Rajavel et al. [11] present a stochastic neighbor embedding (SNE) feature extracting technique with a view to removing unnecessary noise and dimensional reduction from the fundus images. Once the extraction of features is done, the presented optimized deep belief network (O-DBN) classification method can measure the image features into different classes that provide the severity level of DR disease. The researchers in [12] devise a DL-enabled optimized feature selection technique for classifying the phase of DR severity from the fundus image. The candidate lesion regions are identified with the help of an Attention-based Fusion Network (AFU-Net). Afterward, texture and shape features were derived, and consequently, optimum feature subset was chosen by making use of the Improved Harris Hawk Optimizing technique. At last, a deep CNN categorizes the DR phases, and the model weight can be updated through the same technique. In [13], modelled an Autoregressive-Henry Gas Sailfish Optimization (Ar-HGSO)-related DL method for identifying DR and severity level classifiers of DR and Macular Edema (ME) related to color fundus images. The segmenting procedure becomes highly essential for correct identification and classifying procedure that segregates the image into several subgroups. The DL technique can be used for effectual detection of DR and severity classification of ME and DR. Further, the DL approach can be well-trained by the proposed Ar-HGSO method to gain superior outcomes. Aljehane [14] presents an intelligent moth flame optimization with Inception network-based DR detection and grading (IMFO-INDR) approach. The aim of this IMFO-INDR algorithm was to identify the presence of lesions from the fundus image and allot suitable class labels to it. Inception v4 method can be implemented as extracting feature and the hyper-parameters indulged in it were done optimal tuning by using MFO approach. Finally, SoftMax classifier can be employed for allocating class labels to the input fundus images. Gunasekaran et al. [15] use RNN for the purpose of retrieving features from deep networks. So, utilizing computational techniques for identifying some ailments automatically becomes effective solution. The author tested and advanced numerous iterations of a DL structure for forecasting the development of DR in diabetic persons who experienced tele retinal DR assessment. A collection of 3-or 1-field color fundus pictures is the input for both iterations. Using the presented DRNN method, advanced detection of the diabetic state has been carried out by HE identified in a blood vessel of eyes. Gupta et al. [16] project an Optimal Deep CNN for Retinal Fundus Image Classification (ODCNN-RFIC) approach. The proposed method includes preprocessing in 2 stages they are Adaptive Median Filter (AMF) and Guided Filter (GF). The U-Net method was used for segmenting images, permitting the detection of infected regions appropriately. In [17], a new 2-phaseGlaucomaDiagnosisNetwork (ODGNet) and Optic Disk localization were presented. In the initial stage, a visual saliency map merged with shallow CNN can be employed for effective OD localizing from the fundus images In the second stage, the TL-related pre-trained methods were employed for glaucoma diagnosis.

III.METHODOLOGY

In this paper, a novel IoTDL-DRD method was projected for DR detection and classification on retinal fundus images. The presented IoTDL-DRD method allows the IoT devices for data collection purposes and then transfers to the cloud server to process them. Then, the retinal fundus images are preprocessed for noise removal and contrast improvement. Afterward, the MFORG technique was utilized for lesion segmentation in the fundus images. For DR recognition and classification the HBO algorithm with LSTM model is exploited. Figure 1 depicts the block diagram of IoTDL-DRD approach.

A. IMAGE PRE-PROCESSING

At the primary level, the IoT devices capture the retinal fundus images and forward them to the cloud server for further examination. Next, the median filtering (MF) tech nique is used to remove noise and CLAHE is applied to improve contrast level [18]. CLAHE algorithm is extremely effectual in biomedical image analyses and is chiefly utilized for improving the contrast level of an image. This method needs a set of two input parameters such as dimension of clip limit and sub window. In such a way, the presented algorithm recognizes the grid size of window, and also the grid value originated from top left corner area of an image where the computation starts from preliminary index of window.

For FIGURE 1. Block diagram of IoTDL-DRD approach.

27592 every grid point, the histogram of region H I1/2 nearby the image is defined. Then, the histogram is presented over the level of estimated clip limit is trimmed and the Cumulative Distributive Function (CDF) is evaluated. The CDF is evaluated for pixel and the value based on 0 to 255. Following, for all the pixels, the four nearby neighboring grid points should be found. By employing the intensity rate, viz, the pixel index, and the mapping functions of the 4 grid points, CDF measure is evaluated. However the procedure is ended, still it accomplishes the concluding index of a window. Computer vision is a subset of the Deep Learning model, enables the computer to possess an elevated level of understanding in the process of video and digital image processing. The proposed IoTDL DRD method imparts the knowledge on the proposed subject matter to the computer vision, such that it can able to detect the diabetics retinopathy more effectively than the diagnosis through the conventional methodologies.

B. IMAGE SEGMENTATION

Once the images are preprocessed, they are passed into the MRORG technique to segment the fundus images. Region growing (RG) is a pixel-based segmentation technique whereby the similarity constraint including intensity, texture, and so on, are taken into account for grouping the pixel into regions [19]. Initially, a collection of pixels is integrated with the help of iteration methodology. Next, the seed pixel is chosen alongside the regions and the group is supported by integrating with neighboring pixel that is corresponding and whereby it increases the region size. The growth of region is ended whether the neighboring pixel doesn't satisfy the similarity constraint and another seed pixel is carefully chosen. Repeat the process until all the pixels in the image belongs to certain regions. In this work, seed point and threshold selection take a decision regard ing the similarity condition because it plays a major part in enhancing the segmentation accuracy. As mammogram suffers from serious intensity variation, a constant threshold selection doesn't permit accurate segmentation. As a result, this work emphasizes increasing the automatic DA method ology for generating an optimal seed point and threshold. The step-wise procedure for region growing model is shown below.

a. Input the abnormal image.
b. Now, 't' characterizes the improved threshold generated using MFO approach
c. Place t as seed point for region growing model.
d. Add four adjacent pixels.
e. Estimate the distance(d) between the neighboring pixels and mean of region intensity.
f. *Execute region growing if d ≤ t on four adjacent pixels and add all if they are't included before in the region and save the coordinate of the new pixel.*
g. Store the mean of novel region and return to step 2 along with executing the region growing method until each pixel is gathered.

MFO is a new heuristic approach to solving complicated nonlinear optimization problems that were developed [20]. It was inclined by

the reproduction process and behavior of MF. In time t, the MF position in a 2D search space is initialized by a = (a1,...,ad)T and b = (b1,...,bd)T, correspondingly, and velocity v = (v1,...,vd)T is allocated to every MF. The objective function (F) defines the performance of MF. In every iteration, the model saves the global positions (gbest) and best personal (pbest). One cycle (Cyc) is the period among the travel time for every visited node, sum of vacation charging, and two charging demands. The fitness function aim is to minimize system total power consumption, the number of cycles, and MC overall distance traveled that maximizes mobile charging vacation time.

$$F = \left(\frac{Cyc}{10^{2\lfloor \log_{10} Cyc \rfloor}} - 1^{-8}\right)^2 + (e_{\min} - 1^{-8})^2 + (e_{thresh} - 1^{-8})^2 + \left(\frac{1}{\tau_{vac}} - 1^{-8}\right)^2 + \left(\frac{D_{total}}{10^{2\lfloor \log_{10} D_{total} \rfloor}} - 1^{-8}\right)^2$$

$$\text{s.t } E_{\min} < e_{\min} < e_{thresh}, E_{\min} = 0.05 \times E_{\max}$$

$$e_{\max} < e_{thresh} < E_{\max}, E_{\max} = 10.8\text{Kj} \quad (1)$$

Every MF location is attuned based on own and neighbor proficiencies. The male MF velocity and position updating are shown below:

$$a_i^{t+1} = a_i^t + V_i^{t+1}$$

$$V_i^{t+1} = g \times V_{ij}^t + x1 e^{-\beta_{np}^2} \left(pbest_{ij} - a_{ij}^t\right) + x_2 e^{-\beta_{ng}^2} \left(gbest_j - a_{ij}^t\right)$$

Though it should remain in nuptial dance, the opti mal male MF upgrades its velocity with the following expression

$$V_i^{t+1} = V_i^t + m \times n$$

$$b_i^{t+1} = b + V_i^{t+1}$$

The female MF location and velocity are upgraded in the following:

$$V_i^{t+1} = \begin{cases} g \times V_{ij}^t + x_2 e^{-\beta_{n_{mf}}^2 (a_{ij}^t - b_{ij}^t)} & if\ f(b_i) > f(a_i) \\ g \times V_{ij}^t + fl \times n & if\ f(b_i) \leq f(a_i) \end{cases}$$

x1 and x2 indicates individual learning variable. g denotes the inertia weight, β refers to distance sight coefficient, m denotes the nuptial dance, and fl characterizes random flight, correspondingly. The Cartesian distance is signified as np and ng, and n shows an arbitrary value between −1 and 1. Male MF is thought to move at a lower velocity in the nuptial dance, while female MF moves at a higher velocity in the arbitrary flight. Parent MF is selected to mate according to the fitness value. Accordingly, the higher the fitness values, the greater the probability of selection. The crossover operator portrays the mating of two MFs in the following: male and female population. Two off springs (children) are generated in the following:

$$M_{child1} = \ominus \times M_{male} + (1 - \ominus) \times M_{female} \quad (7)$$

$$M_{child2} = \ominus \times M_{female} + (1 - \ominus) \times M_{male} \quad (8)$$

M_{Male} signifies the male and M_{female} female parents ⊖ denote an arbitrary value within a provided range whereas the primary velocity of the children is fixed as zero. Afterward estimating the efficiency of the children, the mutation is presented. The model is avoided getting a local minimum by mutating the children. For inducing mutation in Eq. (8), a uniform distribution arbitrary value is included for chosen children.

$$M_{Child'\alpha} = M_{Child\alpha} + \sigma N_\alpha (0, 1) \quad (9)$$

In Eq. (9), σ and Nα denoted the standard deviation and uniform distributions, correspondingly. Also, the mutated children are assessed in terms of efficiency. The mutated children are combined with the non-mutated children, afterward, they are similarly distributed Parent and child population is arranged by efficiency to choose the following generation of MF for optimization.

C. FEATURE EXTRACTION

To derive optimal feature vectors, the DenseNet model is exploited in this study. The simple DenseNet is created by alternating transition and dense blocks followed by a Soft Max classifier and fully connected layer [21]. The dense block is composed of two cascaded convolution layers comprised of batch normalization (BN), convolution, and leaky rectified linear unit (LReLU) layers ‘‘BN-Conv-LReL’’). Initially, the dense block

makes use of 1 × 1 kernel size for producing 4r output feature map whereas the next generate r feature map with 3 × 3 kernel size, where r is a pre-determined constant and set as 32. The dense blocks concatenate r output feature map with the input map, thus resulting in increased number of maps. The transition block comprises average pooling and convolution layers with 2 × 2 pool sizes. Here, the output feature map count in the transition block is similar to input. In this work, ‘‘conv’’ implies a convolution uni;‘‘1 × 1 × 64 conv’’ denotes the convolution layer in the unit that makes use of the 1 × 1 kernel size for producing 64 output feature map;‘‘2 × 2 pool’’ represents an average pooling layer with 2 × 2 pool siz;θ represents the number of concluding output classe;‘‘[·] × ’’ indicates the structure‘‘[·]’’ is cascaded repeatedly for more than one times. There exists one FC layer and twenty three convolution layer that is much shallower than that of the original DenseNet with 121 convolution layers.

D. IMAGE CLASSIFICATION

For DR recognition and classification, the HBO algorithm with LSTM model is exploited in this study. The most important algorithm of DL methods is CNN. In the study, the hybrid amalgamation of LSTM together with CNN is exploited [22]. Honey bees exhibit a variety of complex behaviors in nature, including mating, reproduction, and for aging. Several honey bee-based optimization algorithms have imitated these behaviors. Honey Bees Optimization is a well known algorithm that was inspired by the mating and breeding behavior of honeybees (HBO).The algorithm begins with a single queen that has no family and progresses to the growth of a colony that has families that contain one or more queens. A colony of honey bees can access numerous food sources in expansive fields and can fly up to 11 km to do so. About one-fourth of the colony’s bees work as foragers. Scout bees start the foraging process by looking for promising flower patches. During the harvesting season, a portion of the scout bees are kept by the colony. The scout bees will search farther after discovering a flower patch in the hopes of discovering one that is even better. Randomly, the scout bees look for the best patches. An artificial neural network called Long Short-Term Memory (LSTM) is employed in deep learning and artificial intelligence. LSTM has feedback connections as opposed to typical feedforward neural networks. Such a recurrent neural network (RNN) can process entire data sequences in addition to single data points (such as images). In order to process the consecutive dataset, RNN is broadly employed. The existing input and the previous output are connected to each other through these RNN models. The tanh activation function there by controls it, such that the series state has been taken into account. In time t, the derivative RNNwouldcommunicateandspreadtotimet−1, t−2,...,l, thus resulting in the presence of a multiplicative factor. Gradient disappearance and explosion occur if there exists endless multiplication. In the forward procedure, the input of starting series has negligible or small effects on the later happening sequence, and consequently, it is regarded as a key challenge of loss distance dependency. By familiarizing numerous gating models, LSTM could resolve the problem easily. For a sigmoid operation, the contemporary input in a function Xt and the previous output ht−1 are provided as an input such that values among zero and one are produced, thus defining the existing novel data that could be effortlessly maintained. The comprehensive state Ct of the following moment is attained using input and forget gates, and it is employed for the initiation of the hidden state ht of the subsequent layer, thus establishing the output of the existing units. The description of the output can be performed through the output gate regarding the data attained from the cell state. A sigmoid function similar to input gate that produces a value 0t among zero and one, which illustrates the quantity of cell state data described for projecting them as output. Figure 2 illustrates the design of a standard LSTM layer using appropriate inputs and outputs. For the LSTM, the respective

alliances among the different gates are arithmetically formulated in the subsequent expression

$$z_t = \tanh(W_z[h_{t-1}, X_t] + b_z)$$
$$i_t = sigmoid(W_i[h_{t-1}, X_t] + b_i)$$
$$f_t = sigmoid\left(W_f\,[h_{t-1}, X_t] + b_f\right)$$
$$o_t = sigmoid(W_o[h_{t-1}, X_t] + b_o)$$
$$c_t = f_t \cdot C_{t-1} + i_t \cdot z_t$$
$$h_t = 0_t \cdot \tanh(c_t)$$

At the end stage, the HBO algorithm is exploited for optimal hyper parameter adjustment process. A honeybee (HB) colony could fly up to 11 km for exploiting food sources and might attempt to terminate larger areas with large sources of food [23]. The cycle of forager starts with the hunt by scout bee for enticing flower patch. Once the scout bee discovers the flower patch, they should search in advance to determine the best patch. The scout bee is desperately searching to discover the optimal spots.

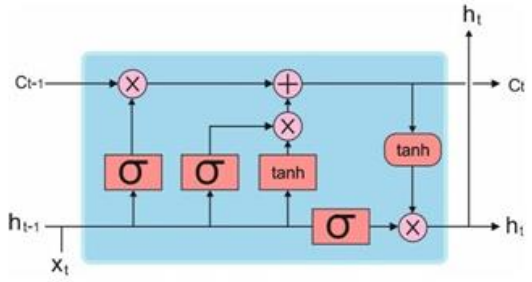

FIGURE 2. Structure of LSTM.

During the hive, the scout bee acts as the counterpart regarding the nature of food sources, on the basis of the sugar content, amongst others. The scout bee injects its nectar and later goes ahead of the hive for celebrating the ballet, termed waggle dance, with others. The waggle dance is modeled afterward the wagging run (the performer makes a loud buzzing rhythm and moves the body simultaneously) that the scout be used to transmit the residual parts of the community data on the food sources. The scout bee offers this data via waggle dance; consistency and distance from the path and hive sources. The waggle direction has eight shaped patterns. First, the scout bees make a noise using their wing muscles which produces a loud buzz, and start to run in a vertical direction in a straight line which indicates the path for sun azimuth at the square and food source location. Instead, scouts circle back and transform left and right. The HBO algorithm derives a Fitness Function (FF) for obtaining enhanced performance of the classification. It sets an optimistic numeral to characterize the good outcome of the candidate solution. The minimization of the classifier error rate has been taken as the FF in this study, as demonstrated in Eq. (11). The worse solution accomplishes the highest error rate and the optimum solution has the lowest error rate.

$$fitness\,(x_i) = Classifier\ Error\ Rate\ (x_i) = \frac{number\ of\ misclassified\ samples}{Total\ number\ of\ samples} * 100 \quad (11)$$

TABLE 1. Pseudocode of HBO algorithm.

ALGORITHM 1: Pseudocode of HBO Algorithm

Instantiation of the parameter value of size of population (N), ps for optimum patch size, ep for elite patch size, fr for the amount of forager bees employed to the elite site, np signifies the amount of forager bees nearby the non-elite optimum patch, nb shows the neighborhood size, Mox characterizes maximal amount of iteration, err denotes error limits.

Express the fitness function.

Order the initialized population based on fitness outcome

Whilek Max or Fitnessvalue Fitnessvaluex-1 ≤ err

K=k+1

For neighborhood search chooses the Elite patch includes the optimal non-elite patch.

Train the foraging bee to the elite patch with non-elite optimal patch.

Inspect every patch of fitness values.

Group the outcome based on the fitness.

Allocate the residual bees for non-optimum location of global search.

Determine the non-optimum patch fitness values.

Arrange the cumulative outcomes based on fitness.

Repeat the process until the ending condition is met.

Stop

IV.SYSTEM ARCHITECTURE DIAGARM:

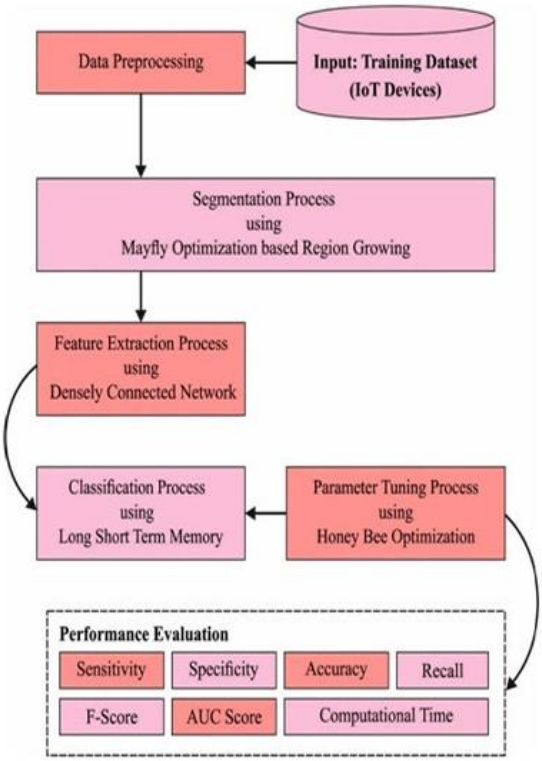

V. RESULT

After preprocessing and augmentation, the dataset was divided into training, validation and testing sets at a ratio of 70:10:20, respectively. After the images were up-sampled using augmentation, the total number of images became 8304 in 4-stage classification. So, the distribution of images across each set is as follows: the training set contains 5978 images (70%), while the validation and testing sets consist of 665 images (10%) and 1661 images (20%), respectively. The number of images per grade of these sets is given in Table 5. For 2-stage classification, out of 4800 images, the training set contains 3456 images (70%), while the validation and testing sets consist of 384 images (10%) and 960 images (20%), respectively. This distribution is shown in Table 6.

VI. DISCUSSION

Two popular databases, namely, Scopus and Web of Science, were used to select papers based on the query already mentioned regarding the data collection under the Methods and Materials section.

Deeper and broader insights were provided through quantitative and qualitative analysis. Both analyses were necessary since they help to form hypotheses for research. Quantitative analysis was done using Excel, VOSviewer, and Biblioshiny. Such a study aims toward and can aid in the evaluation of theories. The qualitative analysis was done regarding a dataset, image segmentation methods, and different machine learning styles ranging from traditional ML styles to deep learning styles used in the literature. It aids researchers in better understanding the automated diabetic retinopathy detection system's motives, necessity, methodology, and justifications. It provides deep insights into various kinds of datasets and suitable methods. Most researchers used publicly available datasets, and few used private datasets collected from the hospital. However, in either case, the issues were as follows:

(i)

First, all images collected belonged to a single modality and were captured from one particular device from one hospital. To overcome such issues, images must be captured from different devices under different circumstances, and multimodal images, such as OCT and fundus images, may be used.

(ii)

Second, fewer DR images may lead to overfitting. Thus, the size of the dataset must be increased, or alternative ML styles, such as semi-supervised, self-supervised, and co-learning techniques, may be used to produce a good model with better performance.

(iii)

The third issue may be due to imbalance, i.e., a biased dataset, which may be avoided by adequately collecting DR images.

In addition to the above, there may be issues of non-uniform illumination and low contrast. Since the eye structure is spherical, it leads to brightness at the center and becomes darker in the surrounding.

Thus, a robust classification model with high accuracy and speed could be possible that considers these points, and hence, can be deployed on a server to be used by ordinary people.

Various image segmentation and ML styles are discussed in this paper. For better segmentation and classification, useful features must be extracted, such as the intensity, statistical, textural, grey-level co-occurrence matrix, moments, standard deviation, and deep features (pixel level and super-pixel level) in the R, G, B, and intensity channels for both greyscale and color images.

VII. CONCLUSION

In this paper, a novel IoTDL-DRD model was developed for DR detection and classification on retinal fundus images. The presented IoTDL-DRD method allows the IoT devices for data collection purposes and then transfers to the cloud server to process them. Then, the retinal fundus images are preprocessed for noise removal and contrast improvement. Afterward, the MFORG technique can be employed for lesion segmentation in the fundus images. For DR recognition and classification, the HBO algorithm with LSTM model is exploited in this study. For evaluating the improved DR diagnostic outcomes of the IoTDL-DRD technique, a comprehensive set of simulations were carried out. A wide ranging comparison study reported the superior performance of the presented model compared to recent state of art approaches. In upcoming years, deep instance segmentation models were derived to boost the classification results. ACKNOWLEDGMENT The authors extend their appreciation to ‘‘the Deputy ship for Research & Innovation, Ministry of Education in Saudi Arabia for funding this research work through the project number G: 693-144-1443’’ and King Abdulaziz University, Deanship of Scientific Research (DSR), Jeddah, Saudi Arabia.

VIII. REFERENCES

[1] S. M. ZOBAED, M. HASSAN, M. U. ISLAM, AND M. E. HAQUE, ‘‘DEEP LEARNING IN IOT-BASED HEALTHCARE APPLICATIONS,’’ IN DEEP LEARNING FOR INTER NET OF THINGS INFRASTRUCTURE. BOCA RATON, FL, USA: CRC PRESS, 2021, PP. 183–2023.

[2] A. Bilal, L. Zhu, A. Deng, H. Lu, and N. Wu, ‘‘AI-based automatic detection and classification of diabetic retinopathy using U-Net and deep learning,’’ Symmetry, vol. 14, no. 7, p. 1427, Jul. 2022.

[3] O. M. Al-Hazaimeh, A. Abu-Ein, N. Tahat, M. Al-Smadi, and M. Al-Nawashi, ‘‘Combining artificial intelligence and image processing for diagnosing diabetic retinopathy in retinal fundus images,’’ Int. J. Online Biomed. Eng., vol. 18, no. 13, pp. 131–151, Oct. 2022.

[4] E. A. REFAEE AND S. SHAMSUDHEEN, ‘‘A COMPUTING SYSTEM THAT INTEGRATES DEEP LEARNING AND THE INTERNET OF THINGS FOR EFFECTIVE DISEASE DIAGNOSIS IN SMART HEALTH CARE SYSTEMS,’’ J. SUPERCOMPUT., VOL. 78, NO. 7, PP. 9285–9306, MAY 2022.

[5] R. Rajavel, B. Sundaramoorthy, K. Gr, S. K. Ravichandran, and K. Leelasankar, ‘‘Cloud-enabled diabetic retinopathy prediction system using optimized deep belief network classifier,’’ J. Ambient Intell. Humanized Comput., vol. 2022, pp. 1–9, Jul. 2022.

[6] A. M. Dayana and W. R. Emmanuel, ‘‘Deep learning enabled optimized feature selection and classification for grading diabetic retinopathy severity in the fundus image,’’ Neural Comput. Appl., vol. 34, pp. 1–21, Jun. 2022.

[7] J. G. R. Elwin, J. Mandala, B. Maram, and R. R. Kumar, ‘‘Ar-HGSO: Autoregressive-Henry gas sailfish optimization enabled deep learning model for diabetic retinopathy detection and severity level classification,’’ Biomed. Signal Process. Control, vol. 77, Aug. 2022, Art. no. 103712.

[8] N. O. Aljehane, ‘‘An intelligent moth flame optimization with inception network for diabetic retinopathy detection and grading,’’ in Proc. 2nd Int. Conf. Comput. Inf. Technol. (ICCIT), Jan. 2022, pp. 370–373.

[9] K. Gunasekaran, R. Pitchai, G. K. Chaitanya, D. Selvaraj, S. A. Sheryl, H. S. Almoallim, S. A. Alharbi, S. S. Raghavan, and B. G. Tesemma, ‘‘A deep learning framework for earlier prediction of diabetic retinopathy from fundus photographs,’’ BioMed Res. Int., vol. 2022, pp. 1–15, Jun. 2022.

[10] I. K. Gupta, A. Choubey, and S. Choubey, ‘‘Mayfly optimization with deep learning enabled retinal fundus image classification model,’’ Comput. Electr. Eng., vol. 102, Sep. 2022, Art. no. 108176.

[11] J. Latif, S. Tu, C. Xiao, S. U. Rehman, A. Imran, and Y. Latif, ‘‘ODGNet: A deep learning model for automated optic disc localization and glaucoma classification using fundus images,’’ Social Netw. Appl. Sci., vol. 4, no. 4, pp. 1–11, Apr. 2022.

[12] N. O. Aljehane, ‘‘An intelligent moth flame optimization with inception network for diabetic retinopathy detection and grading,’’ in Proc. 2nd Int. Conf. Comput. Inf. Technol. (ICCIT), Jan. 2022, pp. 370–373.

[13] R. J. KAVITHA, T. AVUDAIYAPPAN, T. JAYASANKAR, AND J. SELVI, ‘‘INDUSTRIAL INTERNET OF THINGS (IIOT) WITH CLOUD TELEOPHTHALMOLOGY-BASED AGE-RELATED MACULAR DEGENERATION (AMD) DISEASE PREDICTION MODEL,’’ IN SMART SENSORS FOR INDUSTRIAL INTERNET OF THINGS. CHAM,

SWITZERLAND: SPRINGER, 2021, PP. 161–172.

[14] S. Nayak, C. Kumar, S. Tripathi, N. Mohanty, and V. Baral, ''Regression test optimization and prioritization using honey bee optimization algorithm with fuzzy rule base,'' Soft Comput., vol. 25, no. 15, pp. 9925–9942, Aug. 2021.

[15] A. B. TUFAIL, I. ULLAH, W. U. KHAN, M. ASIF, I. AHMAD, Y.-K. MA, R. KHAN, AND M. S. ALI, ''DIAGNOSIS OF DIABETIC RETINOPATHY THROUGH RETINAL FUN DUS IMAGES AND 3D CONVOLUTIONAL NEURAL NETWORKS WITH LIMITED NUMBER OF SAMPLES,'' WIRELESS COMMUN. MOBILE COMPUT., VOL. 2021, PP. 1–15, NOV. 2021.

[16] M. A. M. Shaheen, H. M. Hasanien, M. S. E. Moursi, and A. A. El-Fergany, ''Precise modeling of PEM fuel cell using improved chaotic MayFly optimization algorithm,'' Int. J. Energy Res., vol. 45, no. 13, pp. 18754–18769, Oct. 2021.

[17] T.J.JEBASEELI, J. DAVID, AND V. JEGATHESAN, ''MACHINE LEARNING AND INTERNET OF THINGS TECHNIQUES TO ASSIST THE TYPE I DIABETIC PATIENTS TO PREDICT THE REGULAR OPTIMAL INSULIN DOSAGE,'' IN INTERNET OF MEDICAL THINGS. CHAM, SWITZERLAND: SPRINGER, 2021, PP. 159–174.

[18] N. Gharaibeh, O. M. Al-hazaimeh, A. Abu-Ein, and K. M. Nahar, ''A hybrid SVM Naïve-Bayes classifier for bright lesions recognition in eye fundus images,'' Int. J. Electr. Eng. Informat., vol. 13, no. 3, pp. 530–545, Sep. 2021.

[19] V. Conti, C. Militello, L. Rundo, and S. Vitabile, ''A novel bio-inspired approach for high-performance management in service-oriented net works,'' IEEE Trans. Emerg. Topics Comput., vol. 9, no. 4, pp. 1709–1722, Oct. 2021.

[20] D. S. W. TING, H. LIN, P. RUAMVIBOONSUK, T. Y. WONG, AND D. A. SIM, ''ARTIFICIAL INTELLIGENCE, THE INTERNET OF THINGS, AND VIRTUAL CLINICS: OPHTHAL MOLOGY AT THE DIGITAL TRANSLATION FOREFRONT,'' LANCET DIGIT. HEALTH, VOL. 2, NO. 1, PP. E8–E9, JAN. 2020.

[21] Z. Huang, X. Zhu, M. Ding, and X. Zhang, ''Medical image classification using a light-weighted hybrid neural network based on PCANet and DenseNet,'' IEEE Access, vol. 8, pp. 24697–24712, 2020.

[22] K. PARTHIBAN AND K. VENKATACHALAPATHY, ''INTERNET OF THINGS AND CLOUD ENABLED HYBRID FEATURE EXTRACTION WITH ADAPTIVE NEURO FUZZY INFERENCE SYSTEM FOR DIABETIC RETINOPATHY DIAGNOSIS,'' J. COMPUT. THEOR. NANOSCI., VOL. 17, NO. 12, PP. 5261–5269, DEC. 2020. [3] J. T. KELLY, K. L. CAMPBELL, E. GONG, AND P. SCUFFHAM, ''THE INTERNET OF THINGS: IMPACT AND IMPLICATIONS FOR HEALTH CARE DELIVERY,'' J. MED. INTERNET RES., VOL. 22, NO. 11, NOV. 2020, ART. NO. E20135.

[23] V. RAMALINGAM, D. B. MARIAPPAN, R. GOPAL, AND K. M. BAALAMURUGAN, ''AN EFFECTIVE SOCIAL INTERNET OF THINGS (SIOT) MODEL FOR MALICIOUS NODE DETECTION IN WIRELESS SENSOR NETWORKS,'' IN ARTIFICIAL INTELLIGENCE TECHNIQUES IN IOT SENSOR NETWORKS. BOCA RATON, FL, USA: CRC PRESS, 2020, PP. 181–195.

[24] J. Lei, C. Liu, and D. Jiang, ''Fault diagnosis of wind turbine based on longshort-termmemorynetworks,''Renew.Energy,vol.133,pp. 422–432, Apr. 2019.

[25] X. Ma, T. Yao, M. Hu, Y. Dong, W. Liu, F. Wang, and J. Liu, ''A survey on deep learning empowered IoT applications,'' IEEE Access, vol. 7, pp. 181721–181732, 2019.

[26] N. Gharaibeh, O. M. Al-Hazaimeh, B. Al-Naami, and K. M. Nahar, ''An effective image processing method for detection of diabetic retinopathy diseases from retinal fundus images,'' Int. J. Signal Imag. Syst. Eng., vol. 11, pp. 206–216, Jan. 2018.

[27] M. A. Mohammed, M. K. Abd Ghani, R. I. Hamed, D. A. Ibrahim, and M. K. Abdullah, ''Artificial neural networks for automatic segmentation and identification of nasopharyngeal carcinoma,'' J. Comput. Sci., vol. 21, pp. 263–274, Jul. 2017.

[28] N. Al-Saiyd and S. Talafha, ''Mammographic image enhancement tachniques —A survey,'' Int. J. Comput. Sci. Inf. Technol. Secur., vol. 5, pp. 200–206, Jan. 2015.

[29]X.Zhang,G.Cazuguel,B.Lay,B.Cochener,C.Tron e,andP.Gain,''Feed back on a publicly distributed image database: The Mess id or database,'' Image Anal. Stereol., vol. 33, pp. 231–234, Aug. 2014.